Effect of RF Magnetron Sputtered Nickel Oxide Thin Films as an Anode Buffer Layer in a P₃HT:PCBM Bulk Hetero-Junction Solar Cells

Jwayeon Kim[a,*], Yongkyu Ko[a] and Kyeongsoon Park[b]

[a]Department of Materials Engineering, Hoseo University, Asan, Chungnam 336-795, Republic of Korea
[b]Faculty of Nanotechnology and Advanced Materials, Sejong University, Seoul 143-747, Republic of Korea

Bulk heterojunction solar cells were investigated using poly(3-hexylthiophene) (P₃HT):[6,6]-phenyl-C_{61} butyric acid methyl ester (PCBM) with a nickel oxide (NiO) anode buffer layer between the photoactive layer and an indium tin oxide (ITO) anode layer. The NiO anode buffer layer was deposited using radio frequency magnetron sputtering on an ITO electrode layer for effective hole transport and electron blocking. The NiO film is a p-type semiconductor with resistivity of 0.35 Ω cm. The power conversion efficiency was improved substantially by the NiO anode buffer layer compared to a solar cell with an anode buffer layer made from poly(3,4-ethylenedioxythiophene) (PEDOT):poly(styrene sulfonate) (PSS). The solar cell with a 10 nm thick NiO anode buffer layer had a power conversion efficiency of 4.71%. These results are explained by the improved charge transport across the interface between the active layer and ITO electrode.

1. Introduction

Bulk heterojunction (BHJ) solar cells based on organic materials are very attractive because of their low cost, large area, and light weight [1, 2]. For effective hole transport and electron blocking, PEDOT:PSS has commonly been used as an anode buffer layer (ABL) between an active layer of PCBM and an ITO electrode. However, PEDOT:PSS has problem with causing corrosion to the ITO, as well as non-uniform morphology and instability [3, 4]. Kawano et al. reported that PEDOT:PSS rapidly degrades the performance of a solar cell because of corrosion of the ITO anode electrode from the absorption of humidity in the air [5]. Therefore, it is necessary to develop a new ABL to replace the PEDOT:PSS in P₃HT:PCBM BHJ solar cells.

Suitable ABL materials should have sufficient optical transparency in the visible spectral region. They should also effectively transport holes and block electrons to the anode in a P₃HT:PCBM BHJ solar cell because P₃HT and PCBM are in direct contact with both electrodes. To achieve this, the conduction band energy (E_c) level of the ABL materials (which have p-type semiconductors) should be sufficiently higher than the lowest unoccupied molecular orbital (LUMO) energy level of the PCBM for electron protection. Furthermore, the valence band energy (E_v) level should be near the highest occupied molecular orbital (HOMO) energy of P₃HT for hole transport. There should also be ohmic contact at the interface between the P₃HT and ABL [6, 7].

NiO thin film has received considerable attention recently as a replacement for the PSS:PEDOT ABL in a P₃HT:PCBM BHJ solar cell NiO is a p-type transparent semiconductor with an E_v level of –5.4 eV and E_c level of –1.8 eV. These properties result in effective hole transport and electron blocking [8]. Furthermore, NiO forms ohmic contact with P₃HT.

In the present study, we investigated the effect of a NiO ABL in a P₃HT:PCBM BHJ solar cell. A thin film of NiO was deposited by radio frequency (RF) magnetron sputtering. This method can be used to deposit films on a large area with good adhesion, high deposition, good thickness uniformity and high density [9]. The electrical and optical properties of the NiO film are strongly affected by the sputtering conditions, such as the Ar:O_2 gas flow ratios and thermal annealing temperatures.

2. Experimental

Corning glass (#1737) substrates were first cleaned using sequential ultrasonic baths in acetone, ethanol, and deionized water, followed by drying with an N_2 gun. Presputtering was carried out for 5 min to eliminate contaminants on the target before deposition of the films. NiO films (80 nm) were then deposited on the substrates using RF magnetron sputtering (RF power: 100 W, distance between target and substrate: 10 cm, pressure: 10^{-3} Torr, total gas flow rate: 100 sccm). The deposition was carried out using a target with a diameter of 2 in and various Ar:O_2 gas flow ratios (60:40, 50:50, 40:60, and 30:70) at room temperature in order to obtain optimal NiO films. The films were also deposited with a gas ratio of 30:70 and thermally annealed at 50, 100, 150, and 200 °C at low pressure (10^{-3} Torr, O_2 gas

———
*corresponding author

flow: 100 sccm) to improve the properties. The electrical properties of the films were then measured, including the resistivity, carrier concentration, and the Hall mobility using the Van der Pauw method at room temperature (Ecopia, HMS-3000). The optical transmittance of 10 nm NiO film was measured using a UV-Vis spectrophotometer (Perkin Elmer, Lambda-950) in the range of 300–800 nm. UV photoelectron spectroscopy (UPS) was used to measure E_v level, the Fermi energy (E_f) level, and the energy gap (E_g) of NiO films deposited using $Ar:O_2$ gas flow ratios of 50:50 and 30:70 (UPS: He(I) photon energy: 21.2 eV, Sigma Probe, Thermo VG Scientific).

Solar cells were fabricated on ITO glass (10 Ω/sq) that had been cleaned by sequential ultrasonic baths in acetone, ethanol, and deionized water, followed by drying with an N_2 gun. Different NiO ABLs with thicknesses of 5, 10, and 15 nm were deposited on the ITO glass using RF magnetron sputtering with an $Ar:O_2$ gas flow ratio of 30:70 at room temperature. Thermal annealing was then performed at 200 °C for 10 min in low pressure (10^{-3} Torr, O_2 gas flow: 100 sccm). A PEDOT:PSS ABL was spin coated with a thickness of 100 nm on a different ITO glass substrate, and dried in an oven and exposed to UV ozone for 3 min. The photoactive layers were deposited with thicknesses of 100 nm by spin coating in a glove box and annealed at 140 °C for 20 min on a hot plate under N_2 atmosphere. Then, blended solutions of P_3HT (Sigma-Aldrich):PCBM (Sigma-Aldrich) were prepared in 1,2-dichlorobenzene with a 1:1 mass ratio of P_3HT and PCBM (each 20 mg/ml). The solutions were stirred overnight at 60 °C. Finally, Al cathodes (100 nm) were deposited by thermal evaporation and then thermally annealed for 20 min at 150 °C. The area of the active layer was 0.04 cm². The electrical properties of the solar cells were measured under 100 mW/cm² of illumination (AM 1.5) using a solar cell analyzer (Spectra-Nova Technologies) installed with a xenon lamp. The light intensity of the UV lamp was calibrated using a standard Si photodiode detector.

3. Results and discussion

3.1. Electrical and optical properties of NiO films

The electrical properties of the NiO films (80 nm) deposited at room temperature were measured as a function of the $Ar:O_2$ gas flow ratio. As the $Ar:O_2$ gas flow ratios increased, the resistivity and Hall mobility of the films gradually decreased and the carrier concentration of NiO films gradually increased, as shown in Fig. 1. The resistivity of the film deposited with a ratio of 30:70 was 0.95 Ω cm, which was the lowest value among the samples tested. As the partial oxygen pressure used in the deposition increases, the number of nickel vacancies should increase, and NiO^{2+} is substituted by Ni^{3+} in order to maintain the electro-neutrality, which resulted in a highly doped p-type semiconductor [10].

To decrease the resistivity and increase the transmittance of NiO films deposited with an $Ar:O_2$ flow ratio
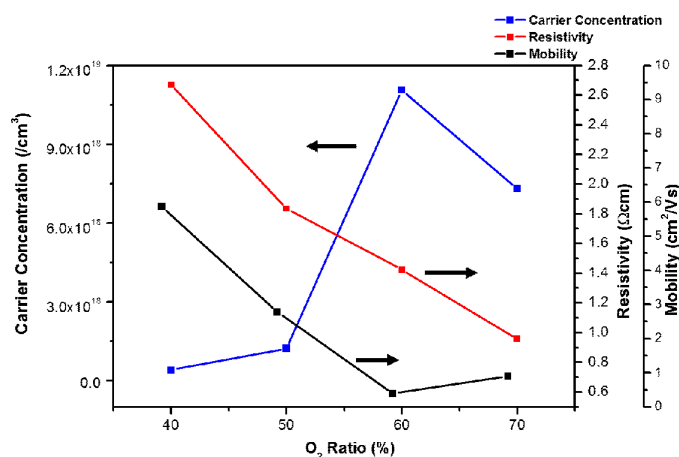
Fig. 1. Electrical properties of 80 nm NiO films deposited at room temperature with different $Ar:O_2$ gas flow ratios.

of 30:70, thermal annealing was carried out for 10 min at 50, 100, and 200 °C at low pressure (10^{-3} Torr, O_2 gas flow ratio: 100 sccm). As the annealing temperature increased, the resistivity and Hall mobility of the NiO films gradually decreased, while the carrier concentration gradually increased, as shown in Fig. 2. The resistivity obtained with annealing at 200 °C was 0.35 Ω cm, which was the lowest value among the tested samples. These process conditions were the best for the NiO deposition in this experiment.
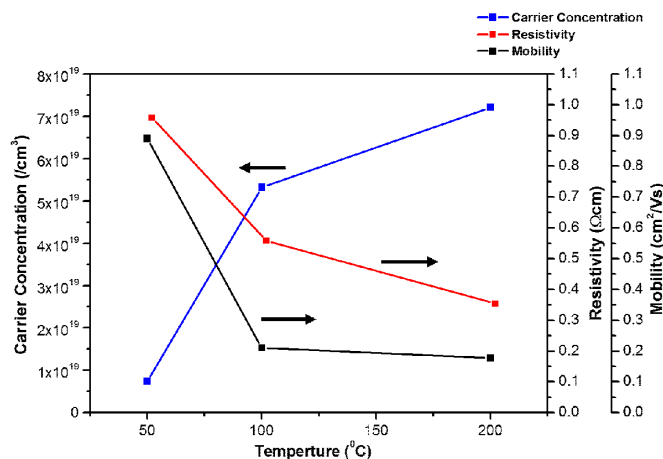
Fig. 2. Electrical properties of 80 nm NiO films deposited with an $Ar:O_2$ gas flow ratio of 30:70 and thermally annealed at 50, 100, and 200 °C for 10 min.

Figure 3 shows the transmittance and E_g values of 10 nm thickness NiO deposited using various $Ar:O_2$ gas flow ratios (70:30, 50:50, 30:70, and 10:90) at room temperature with thermal annealing at 200 °C for 10 min. The average transmittance of the 10 nm NiO films decreased slightly as O_2 gas flow ratios increased, as shown

in Fig. 3. In addition, the E_g values of NiO films decreased from 3.68 to 3.56 eV as the O_2 gas flow ratios increased. The E_g values were calculated using the equation $\alpha h\nu = A(h\nu - E_g)^{1/2}$, where A is the proportionality constant, α is the absorption coefficient, and $h\nu$ is the photon energy (h — Plank's constant, ν — frequency of the photon). The E_g values were obtained by extrapolating the linear portion of the curve to zero absorption [11]. Based on the experimental results, we selected the $Ar:O_2$ flow ratio of 30:70 and thermal annealing at 200 °C for 10 min at low pressure (10^{-3} Torr, O_2 gas flow: 100 sccm) for the ABL. These conditions were optimal for the resistivity, optical transmittance, and E_v level.
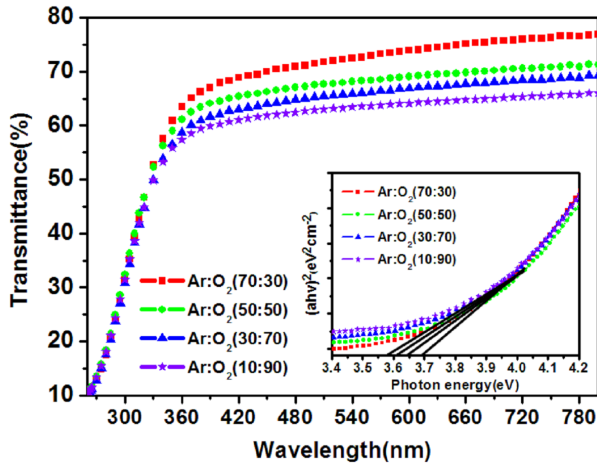
Fig. 3. Optical transmittances and energy band-gaps of 10 nm thick NiO deposited using RF magnetron sputtering with various $Ar:O_2$ gas flow ratios (70:30, 50:50, 30:70, and 10:90) at room temperature and thermally annealed at 200 °C for 10 min.

The NiO film obtained at 30:70 had a little lower optical transmittance than deposited with lower O_2 gas flow ratios (70:30 and 50:50). Nevertheless, the resistivity and E_g value were also lower. When the E_v level of the NiO film is lower than the HOMO energy level of P_3HT, the hole carriers generated in the P_3HT layer have an energy barrier between the P_3HT and NiO ABL. However, when the E_v level of the NiO film approaches the HOMO energy level of P_3HT, the hole carriers are easier to transport from the P_3HT to the NiO ABL. This is possible when E_g value of the NiO films decreases as the O_2 gas flow ratios increase in the NiO deposition process.

Figure 4 shows the UPS spectra (He(I) photon energy: 21.2 eV) of NiO films deposited with $Ar:O_2$ flow ratios of 50:50 and of 30:70, and then thermally annealed at 200 °C for 10 min. The E_v level (–5.1 eV) of the NiO film deposited with a gas flow ratio of 30:70 was higher than that (–5.3 eV) obtained with a ratio of 50:50.

3.2. $P_3HT:PCBM$ BHJ solar cell characterization

$P_3HT:PCBM$ BHJ solar cells were fabricated with NiO ABLs (5, 10, and 15 nm) deposited with an $Ar:O_2$ flow
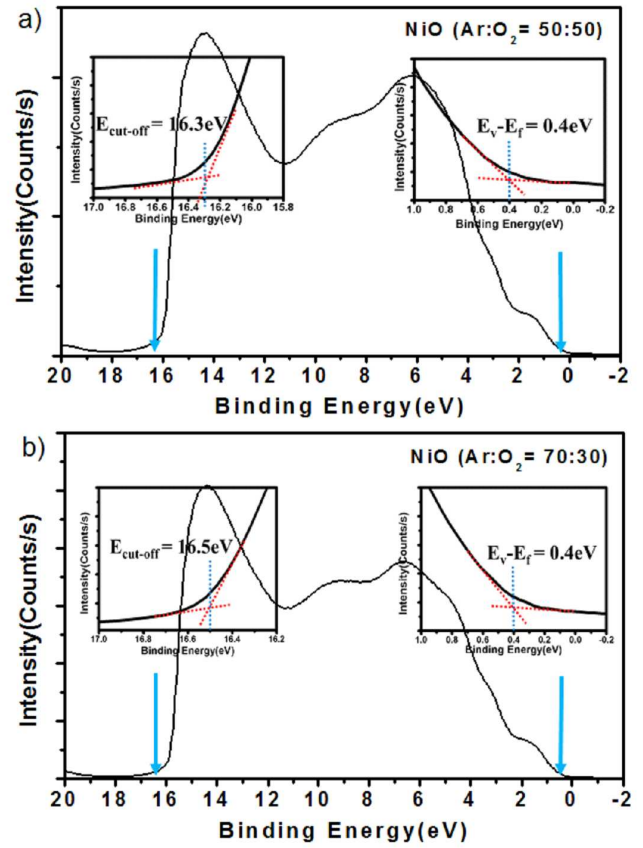
Fig. 4. UPS spectra of NiO films deposited using RF magnetron sputtering with $Ar:O_2$ gas flow ratios of (a) 50:50 and (b) 30:70 and thermally annealed at 200 °C for 10 min.

ratio of 30:70 and thermal annealing at 200 °C for 10 min. Solar cells were also fabricated using a PEDOT:PSS p-type ABL. The process conditions were the same except for the ABL process. Figure 5 shows the current density–voltage plots of the fabricated solar cells. The electrical parameters of the solar cells are summarized in Table I. For the solar cell fabricated with the PEDOT:PSS ABL, open-circuit voltage (V_{oc}), short-circuit current density (J_{sc}), fill factor (FF), and power conversion efficiency (PCE) were 0.69 V, 7.3 mA, 44%, and 3.03%, respectively. The V_{oc}, J_{sc}, and PCE values of the solar cell fabricated with 10 NiO ABL were 0.75 V, 14.3 mA, and 4.71%, respectively, which are higher than those obtained with the PEDOT:PSS ABL. Thus, the data indicate that replacing the PEDOT:PSS with the NiO ABL is feasible. The J_{sc} (14.3 mA/cm^2) value obtained with the 10 nm NiO ABL was much higher than previously reported values [12, 13].

The energy levels of the materials used are shown in Fig. 6. p-type NiO is generally known to have a wide band gap, with E_f level of –5 eV and E_v level of –5.4 eV [14]. The E_v level of NiO film deposited with an $Ar:O_2$ gas flow ratio of 50:50 was –5.3 eV, while that
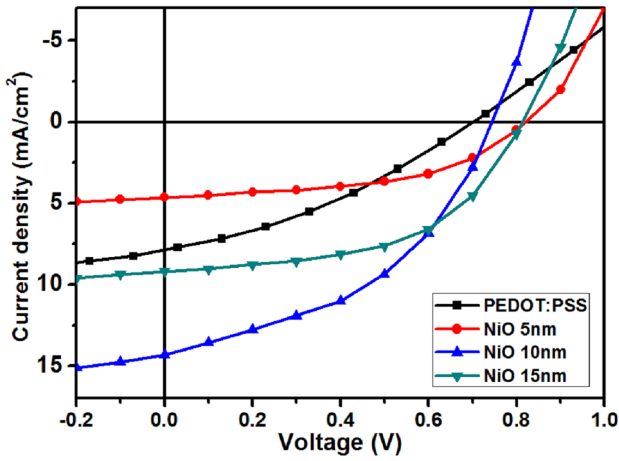
Fig. 5. Current density–voltage plots of P$_3$HT:PCBM BHJ solar cells fabricated with 5, 10, and 15 nm thickness NiO ABLs deposited using RF magnetron sputtering with an Ar:O$_2$ gas flow ratio of 30:70 and thermally annealed at 200 °C for 10 min, as well as PEDOT:PSS (100 nm) anode buffer layers.
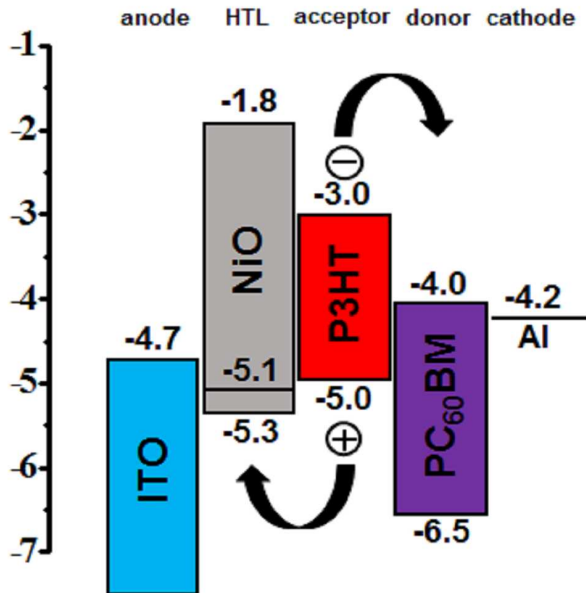
Fig. 6. Energy level diagram of a P$_3$HT:PCBM BHJ solar cell with a NiO anode buffer layer.

obtained at 30:70 was –5.1 eV as shown in Fig. 4. The E_v levels increased with the O$_2$ flow ratios. The E_v level of the NiO ABL obtained with a ratio of 30:70 was near the HOMO energy level (≈ 0.1 below E_f) of P$_3$HT, as shown in Fig. 4. When E_v level of the NiO ABL is close to the HOMO energy level of P$_3$HT, the holes generated at the HOMO energy level of P$_3$HT are transported more easily to the E_v of the NiO ABL. The LUMO energy level (–1.8 eV) of NiO is higher than that of PCBM (–4.0 eV), as shown in Fig. 6 [14]. Thus, the transport of electrons

TABLE I

Electrical parameters of P$_3$HT:PCBM BHJ solar cells fabricated with 5, 10, and 15 nm thickness NiO ABLs deposited using RF magnetron sputtering with an Ar:O$_2$ gas flow ratio of 30:70 and thermally annealed at 200 °C for 10 min, as well as PEDOT:PSS (100 nm) anode buffer layers.

Film thickness [nm]	V_{OC} [V]	J_{SC} [$\frac{mA}{cm^2}$]	FF [%]	PCE [%]	R_S [Ω]	R_{Sh} [Ω]
PEDOT: PSS (100)	0.69	7.3	44	3.03	246	2330
NiO (5)	0.82	4.65	50	1.90	1008	420
NiO (10)	0.75	14.3	44	4.71	388	2996
NiO (15)	0.82	9.18	53	3.96	655	17476

generated from the PCBM to the ITO electrode would be prevented with the NiO ABL.

The solar cell fabricated with a 10 nm NiO ABL had a much higher J_{sc} (14.3 mA/cm^2) than those of the other samples 4.65 mA/cm^2 (5 nm) and 9.18 mA/cm^2 (15 nm). However, FF for the 10 nm ABL (44%) was lower than the other samples of 50% (5 nm) and 53% (15 nm). PCE obtained with the 10 nm NiO ABL (4.71%) was higher than those obtained with thickness of 5 (1.9%) and 15 nm (3.96%). When the NiO film thickness is 5 nm, the layer might not completely cover the ITO substrate. Therefore, the parallel resistance (420 Ω) was lower for this thickness than for the 10 nm (2996 Ω) and 15 nm NiO ABLs (17476 Ω), which fully covered the ITO substrate, as shown in Table I. The PCE is very low when the NiO film thickness is less than 8 nm, which is attributed to the large leakage current and insufficient electron blocking [15]. The PCE of solar cell obtained with the 10 nm NiO ABL was higher than that obtained with the 15 nm NiO ABL. This was probably due to the difference in series resistance between the 10 nm (388 Ω) and 15 nm (655 Ω) layers.

4. Conclusions

We have investigated NiO thin films obtained using RF magnetron sputtering with different gas flow ratios of Ar:O$_2$ and thermal annealing temperatures to replace PEDOT:PSS ABLs in P$_3$HT: PCBM BHJ solar cells. PCE was much improved when using the 1 nm thickness NiO ABL (471%) compared to that obtained using the PEDOT:PSS ABL (3.03%). For the 10 nm NiO ABL obtained with an gas flow ratio of 30:70 and thermally annealed at 200 °C for 10 min, the E_v level was close to the HOMO energy level (≈ 0.1 below of E_f) of P$_3$HT. Therefore, the holes generated at the HOMO energy level of the P$_3$HT would transport easily to E_v of the NiO ABL. These results show that the NiO ABL could replace the PEDOT:PSS ABL in P$_3$HT: PCBM BHJ solar cells.

References

[1] H.-L. Yip, S.K. Hau, N.S. Baek, A.K.-Y. Jen, *Appl. Phys. Lett.* **92, 193313-1 (2008)**.

[2] B.C. Thompson, J.M.J. Frechet, *Chem. Int. Ed.* **47**, 58 (2008).

[3] H.-K. Park, J.-W. Kang, S.-I. Na, D.-Y. Kim, H.-K. Kim, *Sol. Energy Mater. Sol. Cells* **93**, 1994 (2009).

[4] F.C. Krebs, T. Tromholt, M. Jorgensen, *Nanoscale* **2**, 873 (2010).

[5] K. Kawano, R. Pacios, D. Poplavskyy, J. Nelson, D.D.C. Bradley, J.R. Durrant, *Sol. Energy Mater. Sol. Cells* **90**, 3520 (2000).

[6] V. Shrotriya, G. Li, Y. Yao, C-W. Chu, Y. Yang, *Appl. Phys. Lett.* **88**, 073508 (2006).

[7] M.S. White, D.C. Olson, S.E. Shaheen, N. Kopidakis, D.S. Ginley, *Appl. Phys. Lett.* **89**, 143517 (2006).

[8] K.X. Steirer, J.P. Chesin, N.E. Widjonarko, J.J. Berry, A. Miedaner, D.S. Ginley, D.C. Olson, *Org. Electr.* **11**, 1414 (2010).

[9] K. Ellmer, *J. Phys. D Appl. Phys.* **33**, R17 (2000).

[10] S. Seo, M.J. Lee, D.H. Seo, E.J. Jeoung, D.-S. Suh, Y.S. Joung, I.K. Yoo, I.R. Hwang, S.H. Kim, I.S. Byun, J.-S. Choi, B.H. Park, *Appl. Phys. Lett.* **85**, 5655 (2004).

[11] J. Tauc, R. Grigorovici, A. Vancu, *Phys. Status Solidi B* **15**, 627 (1966).

[12] R. Betancur, M. Maymo, X. Elias, L.T. Vuong, J. Martorell, *Sol. Energy Mater. Sol. Cells* **95**, 735 (2011).

[13] D.T. Nguyen, A. Ferrec, J. Keraudy, J.C. Bernede, N. Stephant, L. Cattin, P.-Y. Jouan, *Appl. Surf. Sci.* **311**, 110 (2014).

[14] N. Sun, G. Fang, P. Qin, Q. Zheng, M. Wang, X. Fan, F. Cheng, J. Wan, X. Zhao, *Sol. Energy Mater. Sol. Cells* **94**, 2328 (2010).

[15] N. Sun, G. Fang, P. Qin, Q. Zheng, M. Wang, X. Fan, F. Cheng, J. Wan, X. Zhao, *Sol. Energy Mater. Sol. Cells* **94**, 2328 (2010).